catalysts

MDPI

Article

Direct Hydrogen Production from Extra-Heavy Crude Oil under Supercritical Water Conditions Using a Catalytic (Ni-Co/Al_2O_3) Upgrading Process

Richard Djimasbe [1,*], Ildar R. Ilyasov [2], Michael Kwofie [1], Mohammed A. Khelkhal [1], Dmitrii A. Emelianov [1,*], Ameen A. Al-Muntaser [1], Muneer A. Suwaid [1] and Mikhail A. Varfolomeev [1,*]

[1] Department of Petroleum Engineering, Kazan Federal University, Kazan 420008, Russia
[2] Department of Physical Chemistry, Alexander Butlerov Chemistry Institute, Kazan Federal University, Kazan 420008, Russia
* Correspondence: richarddjimasbe@yahoo.fr (R.D.); dima_emelyan@mail.ru (D.A.E.); vma.ksu@gmail.com (M.A.V.)

Abstract: The generation of hydrogen from unconventional oil is expected to increase significantly during the next decade. It is commonly known that hydrogen is an environmentally friendly alternative fuel, and its production would partially cover the gap in energy market requirements. However, developing new cheap catalysts for its production from crude oil is still a challenging area in the field of petroleum and the petrochemical industry. This study presents a new approach to synthesizing and applying promising catalysts based on Ni, Co, and Ni-Co alloys that are supported by aluminum oxide Al_2O_3 in the production of hydrogen from extra-heavy crude oil in the Tahe Oil Field (China), in the presence of supercritical water (SCW). The obtained catalysts were characterized via scanning electron microscopy (SEM), Brunauer-Emmett-Teller (BET) surface area analysis, transmission electron microscopy (TEM), and, X-ray diffraction analysis (XRD). The obtained XRD data showed 3.22% of Co^{2+} in the Co/Al_2O_4 catalyst, 10.89% of Ni^{2+} in the Ni/Al_2O_4 catalyst, and 1.51% of Co^{2+} and 2.42% of Ni^{2+} in the Ni-CoAl_2O_3 bimetallic catalyst. The BET measurements of the obtained catalysts showed a surface area ranging from 3.04 to 162 m^2/g, an average particle size ranging from 0.037 to 0.944 µm, and micropore volumes ranging from 0.000377 to 0.004882 cm^3/g. The thermal, SCW, and catalytic upgrading processes of the studied samples were conducted in a discontinuous autoclave reactor for 2 h at a temperature of 420 °C. The obtained results revealed that thermal upgrading yielded 1.059 mol.% of H_2, and SCW led to 6.132 mol.% of H_2; meanwhile, the presence of Ni-CoAl_2O_3 provided the maximal rate of hydrogen generation with 11.783 mol.%. Moreover, Ni-CoAl_2O_3 and NiAl_2O_3 catalysts have been found to possess good affinity and selectivity toward H_2 (11.783 mol.%) and methane CH_4 (40.541 mol.%). According to our results, the presence of SCW increases the yield of upgraded oil (from 34.68 wt.% to 58.83 wt.%) while decreasing the amount of coke (from 51.02 wt.% to 33.64 wt.%) due to the significant amount of hydrogen generation in the reaction zone, which reduces free-radical recombination, and thus, improves oil recovery. Moreover, the combination of SCW and the synthetized catalysts resulted in a significant decrease in asphaltene content in the upgraded oil, from 28% to 2%, as a result of the good redistribution of hydrogen over carbons (H/C) during the upgrading processes, where it increased from 1.39 to 1.41 in the presence of SCW and reached 1.63 in the presence of the Ni-CoAl_2O_3 catalyst. According to the XRD results of the transformed form of catalysts ($CoNi_3S_4$), after thermal processing, heteroatom removal from extra-heavy crude oil via oxidative and adsorptive desulfurization processes is promoted. These findings contribute to the expanding body of knowledge on hydrogen production from in situ unconventional oil upgrading.

Keywords: extra-heavy oil; supercritical water; aquathermolysis; catalysts; nickel; cobalt; aluminum oxide; EOR; hydrogen

check for updates

Citation: Djimasbe, R.; Ilyasov, I.R.; Kwofie, M.; Khelkhal, M.A.; Emelianov, D.A.; Al-Muntaser, A.A.; Suwaid, M.A.; Varfolomeev, M.A. Direct Hydrogen Production from Extra-Heavy Crude Oil under Supercritical Water Conditions Using a Catalytic (Ni-Co/Al_2O_3) Upgrading Process. *Catalysts* **2022**, *12*, 1183. https://doi.org/10.3390/catal12101183

Academic Editor: Arturo Martínez-Arias

Received: 15 September 2022
Accepted: 3 October 2022
Published: 6 October 2022

Publisher's Note: MDPI stays neutral with regard to jurisdictional claims in published maps and institutional affiliations.

Copyright: © 2022 by the authors. Licensee MDPI, Basel, Switzerland. This article is an open access article distributed under the terms and conditions of the Creative Commons Attribution (CC BY) license (https://creativecommons.org/licenses/by/4.0/).

1. Introduction

According to the global energy outlook, energy demand will continue to rise and may reach approximately 53% by 2030 [1]. However, according to the EIA, by 2050, hydrogen generation will account for 10% of total final energy consumption [2]. The future of hydrogen fuel generation will not only partially compensate for energy demand, but will also allow us to combat the environmental impact of greenhouse emissions [3]. Although hydrogen generation is intriguing, there is still a lack of interest in creating efficient and acceptable strategies to increase its production and processing from unconventional oil, biomass, or water [4]. It is well known that hydrogen may be created through several petrochemical processes such as hydrocarbon reforming, steam reforming, and partial oxidation [5]. The hydrocarbon reforming process is one of the oldest processes for producing hydrogen. It is an endothermic process that requires an external heat source and may create monoxide and dioxide carbon with a 3:1 hydrogen to monoxide carbon (H_2/CO) ratio. Furthermore, this procedure is commonly applied on an industrial scale and is carried out in a variety of reactors with high and low temperatures. In other words, high-temperature hydrogen production requires temperatures greater than 350 °C in the presence of iron-based catalysts. In the presence of copper-based catalysts, low-temperature generation needs temperatures ranging from 210 to 330 °C [6,7]. For most common hydrocarbons, steam reforming is a fuel refining process that needs temperatures ranging from 180 °C to more than 500 °C. It is commonly regarded as one of the most effective techniques for producing hydrogen at higher heating values, with an efficiency of more than 80–85% when methane is used as feedstock. [8,9].

A significant portion of the scientific community considers partial oxidation (PO) and catalytic partial oxidation (CPO) of hydrocarbons as promising strategies for commercial hydrogen generation, such as automobile fuel cells and other uses. Non-catalytic partial oxidation of hydrocarbons in the presence of oxygen is normally carried out at flame temperatures ranging from 1300 to 1500 °C to achieve full conversion and carbon reduction [5,10]. Biomasses are thought to be the most plausible renewable organic alternative for petroleum [11,12]. The creation of hydrogen from the aforementioned sources relies on several methods such as gasification, pyrolysis, and conversion to liquid fuels via supercritical extraction, liquefaction, hydrolysis, and so on. Biomass and coal gasification rely heavily on partial oxidation of these materials to produce gaseous products (H_2, CH_4, CO, CO_2, and N_2) [13]. As a result, adding steam and/or oxygen to the gasification process would result in steam reforming and a syngas stream with a 2:1 H_2/CO ratio [10,14]. Additionally, it was discovered that superheated steam (800–1000 °C) may be utilized to reform dry biomass, resulting in large hydrogen yields [14].

Downstream hydrogen generation from the aforementioned approaches has always been the subject of research. Despite this interest, no one has researched the in situ generation of hydrogen through improved oil recovery technologies during the production of unconventional oil resources in the presence of SCW and nickel- and cobalt-based catalysts, to the best of our knowledge. As a result, the focus of this research will be on the hydrothermal upgrading of unconventional oil sources in supercritical water using bimetallic catalysts for hydrogen generation.

A growing number of studies have discovered that supercritical water (SCW) plays an important role in hydrogen production during in situ upgrading processes due to its ability to dissolve in organic matter, as well as its coolant properties and the excellent "cage effect," which prevents coke formation earlier during thermally enhanced heavy oil recovery [15–17]. Unconventional oil in situ or ex situ upgrading methods in the presence of supercritical water (SCW) can be regarded as effective and acceptable ways for producing not only oil, but also hydrogen, which is expected to play an important part in energy demand soon. SCW is a thermodynamic state of water that exists above its critical conditions (374.3 °C and 22.1 MPa) [18,19]. SCW is also a homogeneous phase in which the phase of the gas–liquid interface vanishes and most hydrogen bonds weaken, affecting diffusion and the dissolving ability [20,21].

The ability of the SCW to behave as a gas and a liquid during heavy oil thermal upgrading processes in the presence of transition metals acting as effective catalysts during cracking and aquathermolysis reactions would effectively intensify synergistically heavy oil upgrading and stimulate dehydrogenation of its components, resulting in a significant additional release of hydrogen. It is also worth noting that employing metal oxides (catalysts) in the upgrading process of extra-heavy oils or petroleum residues from oil refineries or petrochemical industries is regarded as one of the most promising approaches for the ex situ upgrading of heavy hydrocarbons. This approach has the potential to enhance heavy oil transport and treatment operations [22–26].

The use of transition metal-based nanoparticles with single, double, or multiple alloys is now widely regarded as one of the most advanced ways for improving heavy oil and residue upgrading processes [27,28]. Because of their smaller sizes, increased surface area, better dispersity, and catalytic activity, as well as their thermal stability, nanomaterial-based catalysts work well during heavy oil cracking reactions and avoid coke formation earlier. One of the primary benefits of employing nanoparticles is their ease of recycling, which makes them suitable for new catalytic systems in hydrothermal upgrading processes [29–35].

Mohammed et al. [36] investigated the process of heavy oil upgrading in the presence of supercritical water and a ZrO_2-Al_2O_3-FeO_x catalyst in a batch reactor. The authors discovered that hematite converts to magnetite more significantly than magnetite evolves to hematite. It was discovered that the obtained hydrogen from the upgrading process was roughly 8%. However, the extra hydrocarbons depleted the lattice oxygen, causing the catalyst to deactivate. Duan et al. [37] also performed experimental research on the hydrothermal upgrading of crude algal bio-oil in the presence of supercritical water and a Pt/C catalyst. It has been discovered that the presence of Pt/C increases the removal of heteroatoms (O, N, and S) from improved oil. Furthermore, the mobility of the produced oil increased as a result of viscosity reduction. In addition, this study reported about 5.8 wt.% of H_2 production in the composition of the released gases. Recent works conducted by Remón et al. [38] about the SCW effect on bio-oil upgrading processes in the presence of Ni-Co catalysts supported by carbon nanofibers proved that the use of Ni-Co/CNFs in SCW conditions drastically enhances the properties of the original feedstock and yields higher amounts of H_2 production (18.0%). Under similar conditions, Xiaojuan et al. [39] used Ni-$CoAl_2O_3$ for the methane steam reforming process. It was suggested that the Ni-$CoAl_2O_3$ catalyst plays a crucial role in hydrogen production from methane. Despite the considerable effect generated by different transition metals such as Ni-Co, Ni-Mo, and NiW mixtures on various types of feedstock upgrading processes [40–43], until recently, nobody has ever utilized Ni/Al_2O_4, Co/Al_2O_4, and Ni-$CoAl_2O_3$ for hydrogen production from extra-heavy oil upgrading processes. Until now, catalysts have been utilized to produce hydrogen ex situ in petrochemical and refining operations. In light of recent technological advancements in the field of EOR, there is now much concern about the in situ production of hydrogen from heavy and extra-heavy oil in situ upgrading processes. This paper investigates how to stimulate heavy oil upgrading processes by using Ni/Al_2O_4, Co/Al_2O_4, and Ni-$CoAl_2O_3$ catalysts in the presence of SCW. Our understanding of hydrogen generation from extra-heavy oil in situ upgrading procedures is based on a small amount of data. As a result, we used scanning electron microscopy (SEM), transmission electron microscopy (TEM) equipped with energy dispersive X-ray (EDX), and parametric approaches to investigate the influence of several transition metal-based catalysts on heavy oil thermal upgrading under SCW circumstances. Furthermore, the hydrogen (H_2) production was assessed using GC chromatographic methods, whereas the composition and attributes of the examined extra-heavy crude oil and upgraded oil were measured through SARA analysis, chemical elements (CHSN/O), gas chromatography (GC), and GC–MS. The observed results, in our opinion, provide critical evidence of the potential production of hydrogen through unconventional oil in situ hydrothermal upgrading in the presence of SCW and transition metal-based catalysts.

2. Results and Discussion

2.1. Hydrothermal Catalytic Effect on Gaseous Production in the Presence of Catalysts

The thermal upgrading process of extra-heavy oil in the absence of SCW did not show a significant impact on the production of hydrogen, which has been found to equal to only 1.05 mol.%. However, hydrothermal upgrading in the presence of SCW has increased the hydrogen production yield to 6.13 mol.%. Moreover, hydrothermal upgrading in the presence of SCW and the Ni-$CoAl_2O_3$ catalyst revealed an even higher yield of hydrogen production (11.78 mol.%), as shown in Figures 1 and 2. Interestingly, for the hydrothermal experiments of samples S-3, S-4, and S-5 in the presence of SCW and catalysts, the methane (C_1) yield has been found to increase from 9.94 mol.% for the S-1 to reach a maximum of 40.54 mol.% in the presence of Ni/Al_2O_4. Obviously, the released rate of methane has been found to decrease in the presence of the Ni-$CoAl_2O_3$ catalyst. This could be related to methane consumption from steam reforming, which produces hydrogen; consequently, the yield of H_2 would increase more in the S-5 sample. On the other side, the organic gases C_2–C_4 also were found to decrease from sample S-3, which explains how the use of nickel and cobalt catalysts can inhibit the cracking process of C–C bonds. In addition, hydrogen sulfur gas (H_2S) was not detected in the composition of the investigated gases, and the reason can be attributed to the low content of sulfur in the crude oil, as reported in previous works [44,45]. The obtained results point toward an increased trend in carbon dioxide formation of the CO_2 yield during the heavy oil upgrading process in the presence of SCW and catalysts with a maximum yield of 2.20 mol.% in S-4. Thus, the trend of the CO_2 yield depending on the conditions allows us to conclude that the SCW and catalysts are two key factors for initiation of the water–gas shift reaction. Typically, steam reforming is one of the most important approaches for hydrogen production from methane, which requires a high ratio of H_2O/CH_4 [46]. As can be seen from Figure 1, methane has been significantly consumed to generate hydrogen through steam reforming during extra-heavy oil catalytic upgrading in the presence of 2 mol.% of Ni-$CoAl_2O_3$. Consequently, the ratio of H_2/CO reaches a maximum value of 3.68 compared to other samples, which revealed a lower H_2/CO ratio (<2) such as in S-1 (H_2/CO = 1.43), S-2 (H_2/CO = 1.19), S-3 (H_2/CO = 1.90), and S-4 (H_2/CO = 1.65). In their work, Preeti et al. [47] found a higher ratio of synthetic gas (H_2/CO = 3) during steam reforming of methane, whereas the ratio required for the Fischer-Tropsch process or methanol synthesis was found equal to H_2/CO = 2 [48,49].

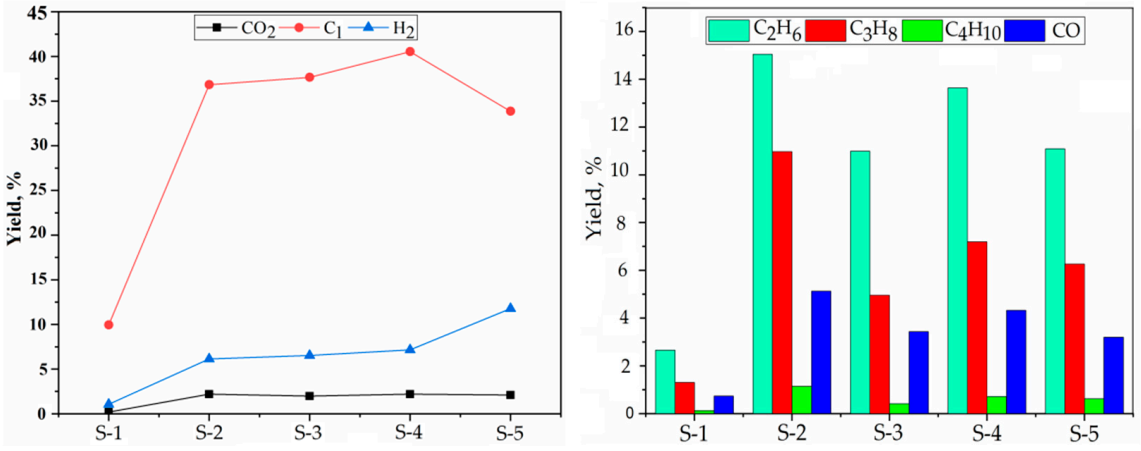


Figure 1. Yield of hydrogen after hydrothermal upgrading of extra-heavy oil.

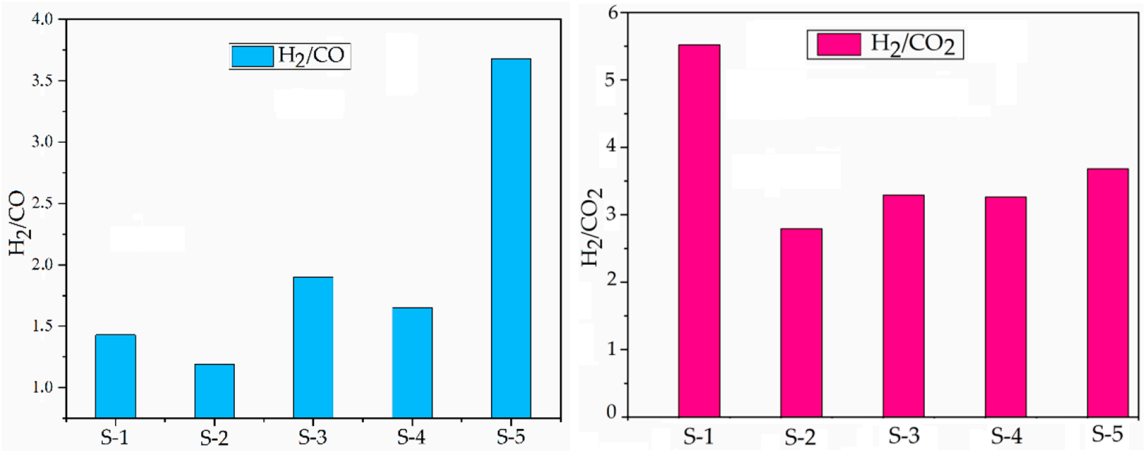


Figure 2. Hydrogen to monoxide carbon ratio after H_2/CO and H_2/CO_2.

2.2. Product Conversion and Distribution in the Upgraded Products

The effect of the opted catalysts and SCW on the extra-heavy oil upgrading process and product distribution is presented in Figure 3. The obtained results revealed that the thermal upgrading of extra-heavy oil without SCW and catalysts is highly characterized by thermal decomposition and a fast recombination reaction of free radicals, which led to a high coke formation (around 51.02 wt.%) and a considerable amount of gases (14.30 wt.%). After 2 h of thermal upgrading, the yield of the upgraded oil reached 34.68 wt.% which is, relatively, considered a low value (see sample S-1 in Figure 3). Yet, the presence of SCW has changed the reaction pathway completely by decreasing the condensation rate of resins and asphaltenes. Furthermore, the obtained results confirmed the crucial role played by SCW in the extra-heavy oil upgrading process, where its presence led to an increase in the yield of the upgraded oil from 34.68 wt.% to 58.83 wt.% and a decrease in the amount of the obtained coke from 51.02 wt.% to 33.64 wt.%. Our findings would seem to suggest that the presence of SCW in S-2 plays an important role in delaying the recombination of the cracked free radicals because it can be, at certain conditions, a source of hydrogen production and a high dispersive agent in the reaction medium. In addition, it can overcome the barrier of mass transfer, which leads, therefore, to decreasing slightly the yield of the released gases from 14.30 wt.% to 7.53 wt.% because of the associated cage effect. The decrease in the released gas yield and the increase in the upgraded oil yield would seem to prove the efficient contribution of SCW in the hydrothermal upgrading reaction because of its dispersive properties (the cage effect), which prevent the early recombination of heavy free radicals [50]. The most striking result to emerge from the obtained data is that using supported catalysts of Ni, Co, and Ni-Co on aluminum oxide could significantly improve the performance of the heavy oil hydrothermal upgrading process (S-3, S-3, and S-3, respectively). The results of heavy oil catalytic upgrading showed that the use of the Co/Al_2O_4 catalyst slightly increased the total yield of released gases from 5.64 wt.% to 8.01 wt.%, whereas the coke formation decreased to 23.97 wt.%. However, the upgraded oil yield was increased to 65.34 wt.%. Besides, a similar effect has been generated from the application of the Ni/Al_2O_4 catalyst in terms of increasing the yield of the upgraded oil, except for a slight increase in released gas content and an insignificant decrease in coke formation. This slight increase in gas yield in the presence of $CoAl_2O_4$ and Ni/Al_2O_4 catalysts is not only related to the high effect of Co and Ni on dehydrogenation reactions and the important role played by Al_2O_3 in the cleavage of C–C bonds, but it is related as well to the yields of C_1, H_2, and CO_2 increasing, which is in complete consistency with the results of Hart Abasari et al. [51]. The obtained results suggest that combining both metals, $Ni\text{-}CoAl_2O_3$, results in a 11.783 mol.% hydrogen yield and a maximum of 72.26 mol.% of upgraded oil. In addition, this combination led to a significant decrease in coke and gas yield.

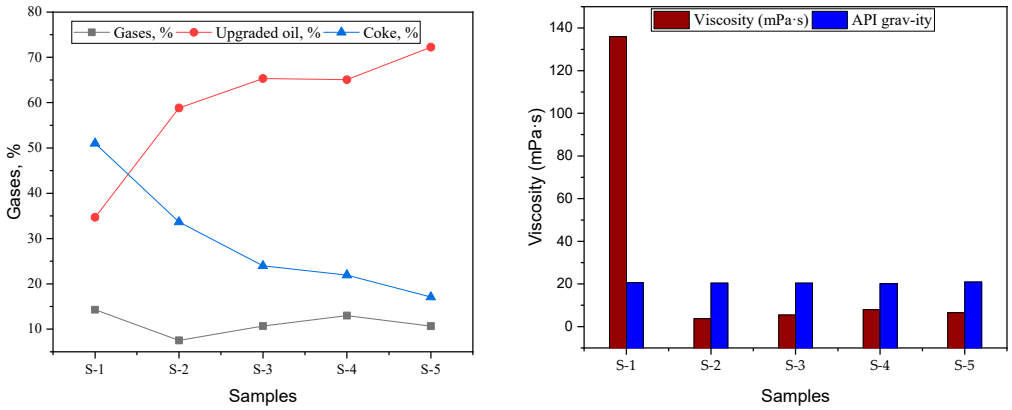


Figure 3. Yield of hydrogen after hydrothermal upgrading of extra-heavy oil.

2.3. SARA Analysis of Initial and Upgraded Oil

The results of the SARA fraction analysis of the initial and upgraded oils are presented in Figure 4. The obtained data revealed that high-molecular-weight molecules break down into light fractions for both catalytic and non-catalytic extra-heavy oil upgrading processes in the presence and absence of SCW.

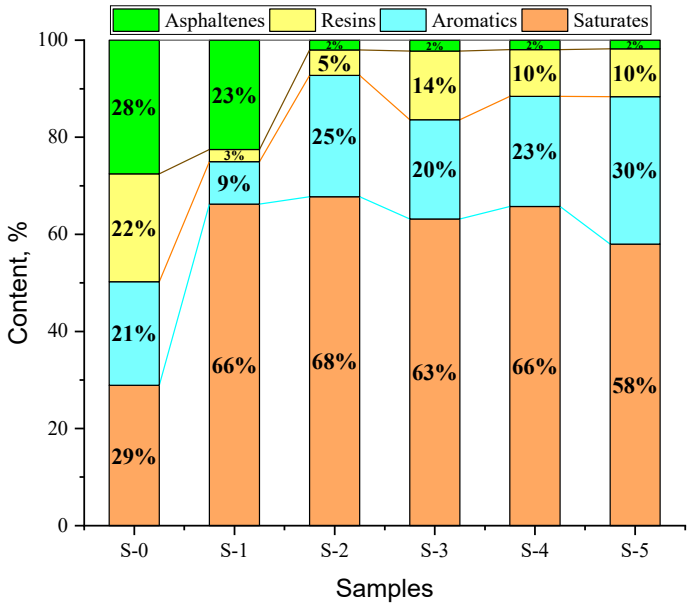


Figure 4. SARA analysis of extra-heavy oil and upgraded oil samples.

2.3.1. Saturate Fractions

The thermal and hydrothermal decomposition of extra-heavy oil in the absence and presence of SCW, and Ni- and Co-based catalysts, showed relatively different impacts on the saturate fractions. As shown in Figure 4, the amount of saturates in the non-catalytic upgraded oil without SCW reached 66 wt.%. This increase in the content of the saturate fraction can be related to the thermal cracking of aromatic, resin, and asphaltene fractions via the cleavage of C–C, C–H, and C heteroatom (S, N, and O) bonds. Another reason would be the dealkylation of alkyl aromatic compounds, as well as of the alkylation reaction of some fragments of saturated molecules. Therefore, the content of aromatics decreased from 21% to 9%, resins from 22% to 3%, and asphaltenes from 28% to 23%. The comparison between heavy oil thermal processing and catalytic thermal processing in the presence of SCW and catalysts showed a different mechanism of the upgrading process. We found that all aromatic fraction content tends to increase because of the possible cyclization of

aliphatic hydrocarbons from saturated fractions. Consequently, the saturate fractions of the samples S-2, S-3, S-4, and S-5 slightly decreased.

2.3.2. Aromatic Fractions

The non-catalytic thermal upgrading of extra-heavy oil has revealed a decrease in aromatic content from 21% to 9%. However, the addition of SCW led to a decrease in the amount by up to 25%; meanwhile, the presence of Ni- and Co-based catalysts led to a decrease in the content less than 20%, followed by a decrease up to 23% and 30%, respectively. The supplementary increase in the content of aromatics observed in the samples of S-2, S-4, and S-5 compared to that of the extra-heavy crude oil reveals a good activity and selectivity of catalysts for cracking, the dehydrogenation of cycloalkanes, and the cyclization of some aliphatic hydrocarbons in the resins and asphaltenes; consequently, the content of the saturate fractions has slightly decreased in the presence of catalysts. On the one hand, the higher dispersity of SCW and its compatibility with hydrocarbons improved most resin and asphaltene transformations into light fractions, which increased the content of the saturated fractions to 68%. On the other hand, the catalysts played a significant role in accelerating not only the conversion of resins, but also that of asphaltenes to aromatics. This dual effect of SCW and catalysts has resulted in a significant decrease in asphaltenes from 28 wt.% to 2 wt.% because of their conversion.

2.3.3. Resin and Asphaltene Fractions

Resins and asphaltenes are the heaviest compounds in extra-heavy crude oil with a complex structure of molecules. It is common knowledge that their presence in thermal or catalytical upgrading processes in the refining units can cause many operational problems, such as aggregation and deposition, because they are widely considered as being the main precursor of coke formation. The decomposition of the resin fraction is most impacted by thermal upgrading, compared to hydrothermal and catalytic upgrading processes (SCW and catalysts). After the thermal and hydrothermal upgrading process of extra-heavy oil, the content of resins decreased from 22% to 3%, and then 5%. However, asphaltenes were not efficiently decomposed during thermal upgrading. It should be noted that the effective decomposition of asphaltenes can only be achieved in the presence of SCW and catalysts. In fact, the significant decrease in resin content (from 22% to 3%) observed during the thermal upgrading process (sample S-1) is related to the simultaneous decomposition and condensation of heavy free radicals to asphaltenes, and then to coke (see Figure 1). Nonetheless, the consumption of resins (from 22% to 5%) observed in the hydrothermal upgrading process in the presence of SCW is proportional to resin conversion into aromatics or saturated fractions. It is worthwhile noting that asphaltenes of the Tahe extra-heavy oil are more thermally stable in the absence of SCW and catalysts. The thermal stability of asphaltenes during non-catalytic thermal upgrading is in complete agreement with the viscosity data which showed high viscosity (135.96 mPa·s) for the sample S-1, compared to that obtained for samples S-0, S-2, to S-5.

2.4. Elemental Analysis of Heavy Oil before and after Thermal, Hydrothermal, and Catalytic Upgrading

Table 1 illustrates the results of the chemical element composition (CHSN/O and Me) analysis of the studied extra-heavy crude oil before and after thermal, hydrothermal, and catalytic upgrading. It has been found that carbon redistribution trends increase in the obtained samples from thermal, hydrothermal, and catalytic upgrading processes. The maximum content of carbon (87.07%) was reached in sample S-2 in the presence of SCW. However, the redistribution of atomic hydrogen over carbon atoms during the upgrading process showed that the thermal upgrading process impacts, mainly, the cracking of C–C only and does not significantly impact the hydrogenation of carbon. This showed that the redistributed hydrogen rate by thermal upgrading does not significantly change in the upgraded oil compared to that of the initial extra-heavy crude oil (from 9.82% to 9.78%).

Furthermore, our results indicated that the presence of SCW coupled with Ni- and Co-based catalysts has significantly improved the oil's properties and composition by increasing the hydrogen rate to 10.26% in the presence of SCW and to 11.69% in the presence of the used catalysts. Moreover, the relative value of H/C also showed that SCW in the presence and absence of Ni/Al_2O_4-, Co/Al_2O_4-, and Ni-CoAl_2O_3-based catalysts can, overall, strengthen the redistribution of the hydrogen content by stimulating hydrogenation reactions. It can cause the ionization of water as well through adsorption. This observation is completely consistent with XRD results of the used catalyst, which highlighted the ionization of water over metals as shown by AlO(OH) compounds (see Figure 14). Water ionization during the catalytic upgrading process of extra-heavy oil can strengthen the supplementary hydrogen generation for upgrading and reducing the coke formation. Additionally, the obtained data from thermal upgrading and hydrothermal upgrading in the presence of SCW and catalysts on the gas composition and elemental analysis highlight a significant gap between molecular H_2 and atomic H. The obtained data showed an increase in the H/C ratio (from 1.39 to 1.41) in the presence of SCW. However, this ratio was found to be higher in the presence of the opted catalysts, where it increased from 1.39 to 1.63. Based on the hydrogen release rate in gaseous products (shown in Figure 14 and composition redistribution in liquid products, we can assume that Ni- and Co-based catalysts can cause both simultaneous reactions of hydrogenation and dehydrogenation during the upgrading process. This phenomenon was also observed in our previous works [52]. It has been found that during the extra-heavy oil catalytic upgrading process, hydrogen production can occur from the accelerated dehydrogenation of water on the surface of the catalyst. Our results indicate that heteroatom and metal (S, N, Me + O) contents also tend to decrease in the obtained samples from thermal and hydrothermal upgrading processes in the presence and absence of catalysts. Sulfur content has significantly decreased from 1.84% in extra-heavy crude oil to 1.42% in sample S-1, and then to 1.35% in sample S-5. The mechanism of sulfur removal from both samples (S-1 and S-5) is supposed to be different. For sample S-1, the sulfur is removed by a radical mechanism, where the resulting free radicals from thermal processing undergo recombination; meanwhile, the high-molecular-weight heteroatomic hydrocarbons occur through polymerization during coke formation. Detecting $CoNi_3S_4$ compounds in XRD patterns of the used catalyst (see Figure 11) points toward the idea that the sulfur removal from extra-heavy oil of sample S-5 during the catalytic upgrading process can take place only by oxidative and adsorptive desulfurization mechanisms. This mechanism is similar to that of the oxygen+metal removal from oil.

Table 1. Results of elemental composition of initial and upgraded oils.

Samples	Chemical Elements, wt.%					
	C	H	S	N	(Me + O) *	H/C
S-0	84.38	9.78	1.84	0.47	3.53	1.39
S-1	87.06	9.82	1.42	0.92	0.78	1.35
S-2	87.07	10.26	1.57	0.69	0.41	1.41
S-3	86.40	10.83	1.53	0.71	0.53	1.50
S-4	86.31	11.03	1.55	0.69	0.42	1.53
S-5	85.85	11.69	1.35	0.68	0.43	1.63

* is determined by difference.

2.5. Aromatic Identification in the Upgraded Oil by GC–MS

Table 2 elucidates the results of the aromatic content analysis in the initial extra-heavy crude oil and the upgraded oil samples obtained from thermal, hydrothermal (SCW), and catalytic processes via GC-MS analysis. The obtained results of GC-MS of the upgraded products are subdivided into mono-, di-, and polyaromatic fractions. According to GC-MS results, the thermal upgrading of extra-heavy oil is characterized by two different pathways: the first includes the C–C thermal cracking reaction, and the second one includes the cleavage of C–S bonds in resin fractions. The obtained data indicate that the content

of n-alkanes increased from 0.67% to 23.30% and the polymerization of diaromatics led to an increase in polyaromatics from 37.46% to 48.98%. Additionally, these results agree with the results of the SARA analysis, which revealed a significant decrease in resins to aromatics and asphaltenes. Moreover, monoaromatic fractions abruptly increased from 4.22% to more than 35% in the presence of SCW, and $CoAl_2O_4$ and Ni-$CoAl_2O_3$ catalysts, at the expense of polyaromatic fractions which decreased from 37.46% to 10%. The significant decrease in polyaromatics contributes to the monoaromatic increase, as indicated by samples S-2, S-4, and S-5. This increase in monoaromatics is related to the conversion of some alkanes and polyaromatic fractions into mono- and diaromatic fractions through the cyclization of aliphatics, and into gaseous products via the hydrothermal and catalytic cracking of asphaltenes, respectively. The obtained data about the significant conversion of polyaromatics into mono- and diaromatic fractions in samples S-2, S-3, and S-5 are in a good agreement with the results obtained in [52–54]. Contrary to samples S-2, S-3, and S-5, samples S-1 and S-4 showed a different effect of the upgrading process on alkane's fraction content, which increased because of cracking and alkylation of aliphatic fragments. The slightly higher content of polyaromatics in samples S-1 and S-4 confirms the results of the upgraded oil's viscosity, which showed slightly higher values than other samples.

Table 2. Composition and content of aromatic fractions of heavy oil and upgraded oil samples.

Compounds	S-0	S-1	S-2	S-3	S-4	S-5
Alkanes	0.67	23.30	2.47	3.01	27.80	0.25
Monoaromatics	4.22	18.05	44.93	35.50	1.75	48.74
Diaromatics	55.61	9.653	35.50	50.58	9.13	34.75
Polyaromatic	37.46	48.98	13.28	10.32	61.32	9.09

3. Experimental Methods

3.1. Materials

The studied extra-heavy crude oil sample in this paper was obtained from Tahe Oil Field and kindly provided by the Sinopec Company (Beijing, China). The sample was extracted from deeper reservoirs at more than 5500 m using a gas injection technique. N-heptane (99.6%), toluene (99.8%), chloroform, and isopropyl alcohol (99.5%) were provided by the Eco.1 Company (Saint-Petersburg, Russia). The characteristics, properties, and composition of the heavy crude oil from the Ashal'cha Oil Deposit can be found in Table 3.

Table 3. Viscosity, density, SARA fractions, and elemental analysis of the studied heavy crude oil.

Viscosity (mPa·s)	API Gravity	SARA Fractions wt.%				Elemental Analysis wt.%			
		S	A	R	A	C	H	N	S
$61 \cdot 10^6$ [a]	4.5	26.11	19.30	20.05	24.90	84.8	9.78	0.33	1.84

[a] Rotational viscometer (Brookfield DV-II Pro) was used according to ASTM D-4124.

3.2. Analytical Methods

The carbon number distribution of the saturate fractions and the composition and yield of evolved gases after hydrothermal upgrading processes, including hydrocarbons gases (C_1–C_4), hydrogen (H_2), hydrogen sulfur (H_2S), monoxide carbon (CO), dioxide carbon (CO_2), and nitrogen (N_2), were determined using Agilent 7890A gas chromatography (GC, Santa Clara, CA, USA) with a flame ionization detector (FID) and gas chromatography (Chromatec Crystal 5000.2, Chromatec, Yoshkar-Ola, Russia), respectively. The viscosity and density of the heavy crude oil and upgraded oil samples [53] were measured via the Brookfield DV-II + Pro (Fungilab, Barcelona, Spain) and SVM 3000t (Anton Paar, Graz, Austria) viscometers [54]. The elemental composition (C, H, N, and S) of the initial and upgraded oil samples was analyzed via the PE 2400 Series II CHNS/O Analyzer

(PerkinElmer, Waltham, MA, USA) [53]. The composition fraction of saturated hydrocarbons, aromatics, resins, and asphaltenes (SARA) was performed according to ASTM D 4124. The aromatic fractions of the heavy crude oil and upgraded oil samples were measured via a gas chromatography/mass spectrometer GC–MS, which included the gas chromatograph, "Chromatec Crystal 5000", with an ISQ mass-selective detector (Thermo Fisher Scientific, Waltham, MA, USA). Xcalibur software (Thermo Fisher Scientific, Waltham, MA, USA) was used to process the results. The chromatograph is equipped with a capillary column that has a 30 m length and 0.25 mm diameter. The rate at which the carrier gas (helium) flow was performed was 1 mL/min. The injector temperature was 310 °C. The thermostat temperature program was as follows: temperature increase from 100 to 150 °C at a rate of 3 °C/min and from 150 to 300 °C at a rate of 12 °C/min, followed by its isotherm until the end of the analysis. The electron energy of the mass detector was 70 eV; the ion source temperature was 250 °C. Compounds were identified through the electronic library of the NIST spectra database and based on data from literature sources [53]. The resin and asphaltene fractions were determined using a Bruker AVANCE-III-HD-500 NMR spectrometer (Bruker, Billerica, MA, USA) [55].

3.3. Synthesis of Catalysts

In order to understand the effect of Ni/Al_2O_4 and Co/Al_2O_4 catalysts, and the catalyst of their alloy $Ni\text{-}CoAl_2O_3$, on heavy oil upgrading and hydrogen generation in SCW conditions, we used 5 g of $Ni(NO_3)_2{\cdot}6H_2O$ to obtain the Ni/Al_2O_4 catalyst, and 5 g of $Co(NO_3)_2{\cdot}6H_2O$ to obtain Co/Al_2O_4. Next, these salts were each dissolved in 15 mL of distilled water. The obtained solutions were separately imprinted on the catalyst support of aluminum oxide (γ-Al_2O_3). The alloy of the $Ni\text{-}CoAl_2O_3$ catalyst, on the other hand, was obtained by dissolving 2.5 g of $Co(NO_3)_2{\cdot}6H_2O$ and 5g of $Ni(NO_3)_2{\cdot}6H_2O$ in 25 mL of distilled water. The resulting aqueous co-solution of $Co(NO_3)_2{\cdot}6H_2O$ and $Ni(NO_3)_2{\cdot}6H_2O$ was then imprinted to aluminum oxide (γ-Al_2O_3) as a catalyst support under 500–600 r/min stirring. All impregnation processes were seated at a constant temperature of 70 °C for 4–6 h. The resulting catalytic complex was treated in the furnace under 150 °C for 24 h. The calcination process of catalysts was then set at 1200 °C for 2 h. The obtained catalysts are presented in Figure 5.



Figure 5. Bimetallic catalysts based on Ni, Co, and γ-Al_2O_3.

3.4. Catalyst Characterization

In order for us to be able to study the structure, morphology, and surface properties of the obtained catalysts, we applied a method of analysis which combined X-ray diffraction (XRD), SEM, TEM, and BET analyses. This method was chosen because it is one of the most practical methods applied in studying catalysts' morphological and structural properties.

3.4.1. XRD Analysis

XRD measurements were carried out on the MD-10 desktop diffractometer (Rodicon, Saint Petersburg, Russia) using Fe Kα radiation (λ = 1.93728 Å) in the Debye–Scherrer geometry. The obtained XRD data of the opted catalysts before and after hydrothermal processing of heavy oil, in addition to coke, are presented in Figures 6 and 7.

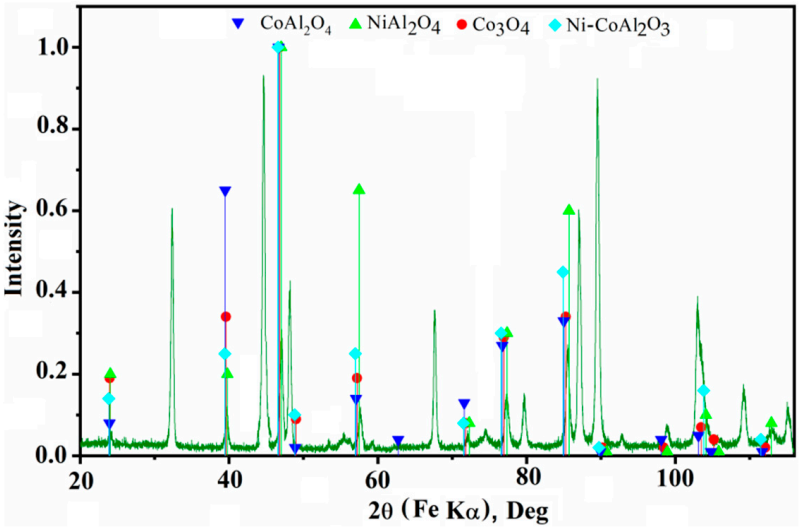


Figure 6. XRD patterns of the obtained catalysts.

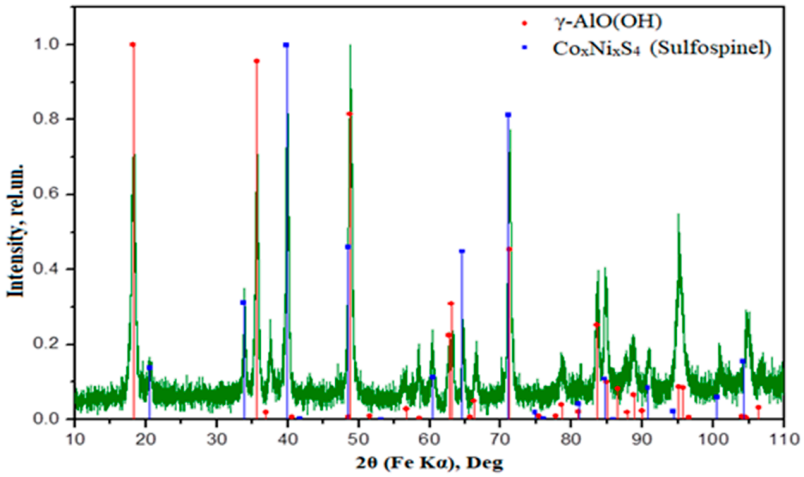


Figure 7. XRD patterns of the fresh catalysts and coke.

3.4.2. SEM/TEM Analyses

In order to study the composition and morphology of the obtained catalysts, we used FESEM (Merlin Carl Zeiss, Oberkochen, Germany) equipped with an Aztec X-MAX energy dispersive spectrometer (Oxford Instruments, Abingdon, UK). The morphological structure and surface analysis were taken at an accelerating voltage of 5 keV and a probe current of 300 pA. Moreover, the microprobe elemental analysis was performed at an accelerating voltage of 20 keV and the sounding depth was about 1 µm. The SEM images and spectra of the obtained catalysts are presented in Figures 8–10.

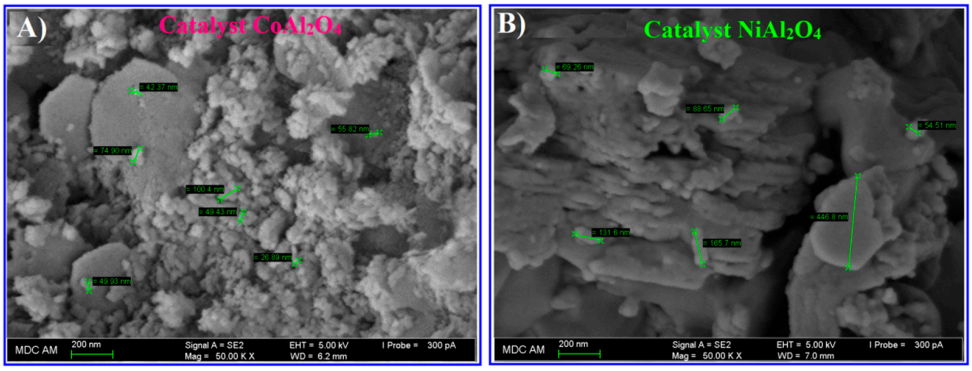


Figure 8. Morphological structure of Co/Al_2O_4 (**A**) and Ni/Al_2O_4 (**B**) catalysts obtained from SEM.

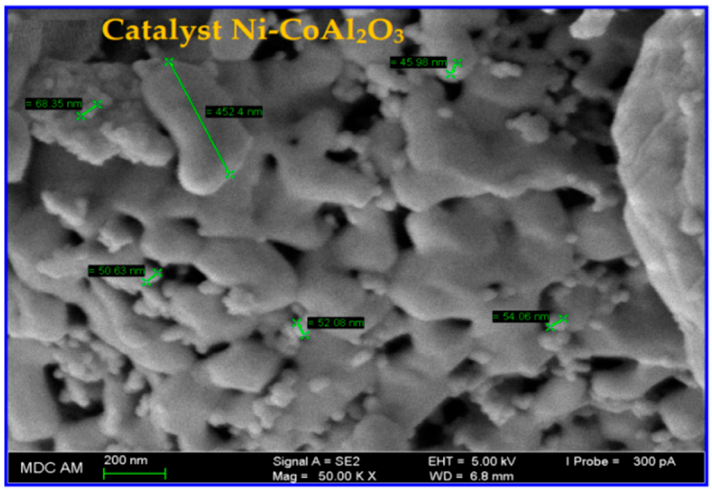


Figure 9. Morphological structure of $Ni\text{-}CoAl_2O_3$ obtained from SEM.

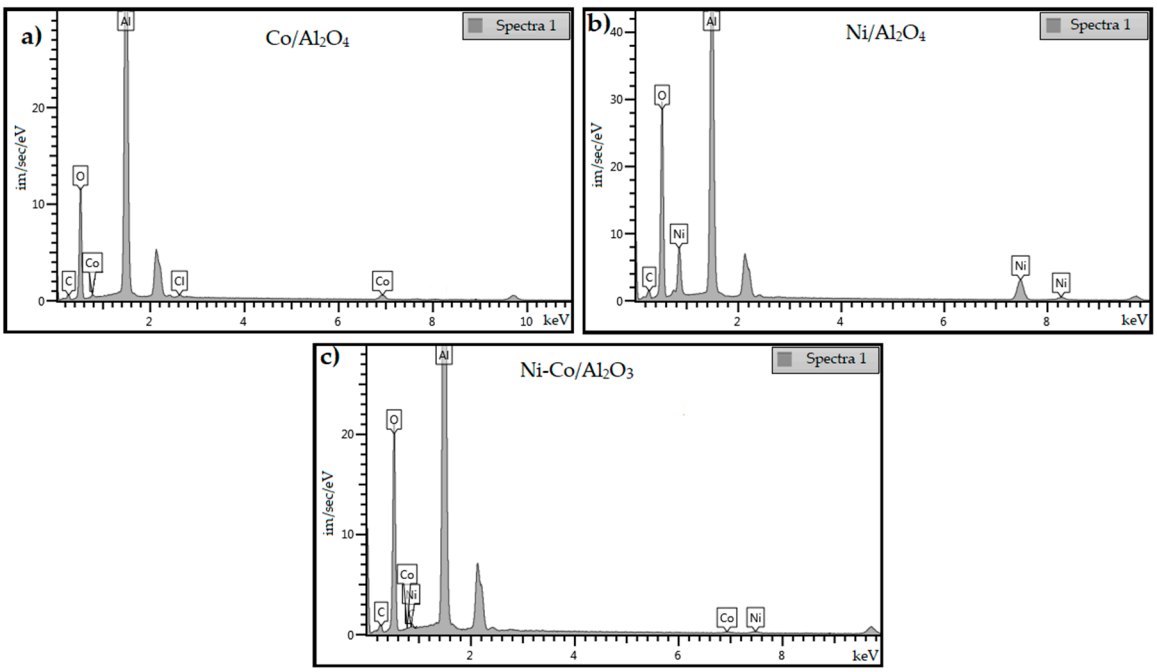


Figure 10. Spectra of Ni- and Co-based catalysts via SEM-EDX analysis ((**a**): for Co/Al2O4, (**b**): for Ni/Al2O4, (**c**): for Ni-Co/Al2O4).

3.4.3. Analyses and Determination of Specific Surface Area and Pore Volume

The specific surface area, pore volumes, and their distribution over pore diameters were determined on an ASAP 2400 analyzer from Micromeritics (Norcross, GA, USA). The value of specific surface area was determined by the thermal desorption of nitrogen with a ±3% measurement accuracy and calculated by assuming the nitrogen molecule's surface area as being equal to 0.162 nm^2. The density of nitrogen in the normal liquid state is 0.808 g/cm^3. Nitrogen adsorption isotherms were obtained at T = −196 °C after sample degassing at T = 500 °C to a residual pressure of 0.013 Pa. The calculations of the parametric volume and the distribution of pore volumes by diameters were carried out using the desorption branch of the isotherm according to the standard Barrett-Joyner-Halenda procedure with a ±13% measurement accuracy.

XRD patterns revealed that the obtained catalysts consist of Co/Al_2O_4, Ni/Al_2O_4, and $Ni\text{-}CoAl_2O_3$ and a non-significant part of Co_3O_4. The obtained data revealed the main features as well in the 2θ range of 30–35°. There are two bands, namely, the γ-band and C [002] band. In analogy with asphaltenes [56], the γ-band is connected to spacing between condensed saturated structures, whereas the C [002] band is connected to spacing between aromatic layers. From the relationship of these bands with each other, we may make the conclusion about the "aromaticity" of petroleum coke. It is seen that the C [002] band is almost absent on the XRD pattern of coke without a catalyst. However, with the addition of the Al_2O_3-based catalyst, this band manifests itself, and has maximal intensity on the XRD pattern of coke with the $Co\text{-}Al_2O_4$ catalyst. We suppose that other small reflexes may be related with sulfides of Ni and Co. A broad reflex at $2\theta \approx 58°$ on XRD patterns of cokes with catalysts may relate to the amorphous form of Al_2O_4.

On the other hand, we used a transmission electron microscope (TEM) Hitachi HT7700 Exalens (Hitachi Ltd. Tokyo, Japan) to illustrate the internal and external morphological structure of the obtained catalyst samples by placing 10 microliters of the suspension on a formvar/carbon lacey 3 mm copper grid, followed by drying at room temperature. After drying, the grid was placed under a transmission electron microscope using a special holder for microanalysis. After that, the analysis was performed at an accelerating voltage of 100 kV in TEM mode. Finally, the elemental analysis was carried out in STEM mode, at the same parameters using the Oxford Instruments X-Max™ 80T detector (Abingdon, UK). The obtained TEM images for the studied catalysts are shown in Figures 11 and 12.

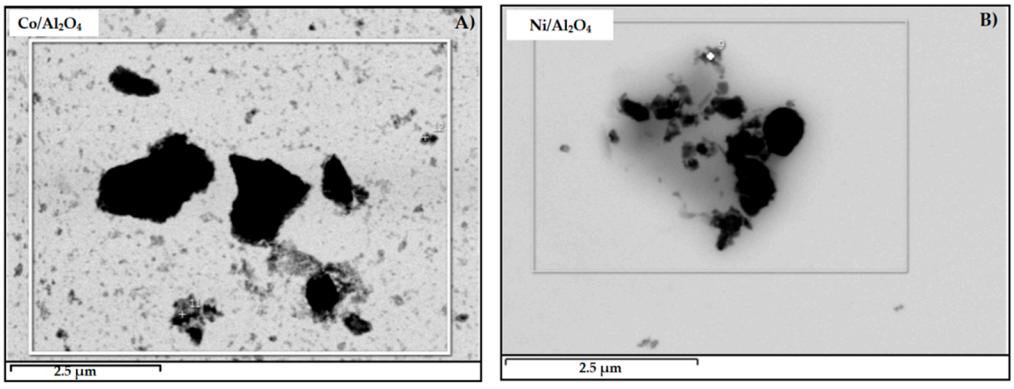


Figure 11. Morphological structure of Co/Al_2O_4 (**A**) and Ni/Al_2O_4 (**B**) obtained from TEM.

SEM and TEM analysis results (Table 4) showed 3.55% of cobalt (Co) in the Co/Al_2O_4 catalyst, and 12.15% of nickel (Ni) in the Ni/Al_2O_4 catalyst. Moreover, the $Ni\text{-}CoAl_2O_3$ alloy catalyst contained 2.71% of Ni and 1.69% of Co.

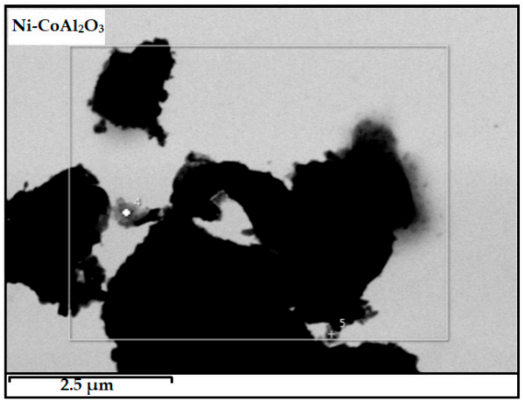


Figure 12. Morphological structure of Ni-$CoAl_2O_3$ obtained from TEM.

Table 4. The chemical composition content of the obtained catalysts.

Catalysts	Nickel (Ni)	Cobalt (Co)	Aluminum Oxide (γ-Al_2O_3)	Oxygen (O_2)
$CoAl_2O_4$	0.00	3.55	54.32	42.11
$NiAl_2O_4$	12.15	0.00	35.52	52.31
Ni-$CoAl_2O_3$	2.71	1.69	46.05	49.53

3.4.4. BJH Adsorption and Desorption of Catalysts

Although the catalysts were synthesized by the same method, the large difference observed in the average sizes also depends on the composition of the catalysts, as can be seen in Table 4. Therefore, the catalyst average particle size is 37.0355, 944.33, and 874.8551 nm (see Table 5). In this article, we investigated the effect of cobalt, nickel, and the cobalt–nickel metal alloy on the refining process of extra-heavy oil. However, it is clear that the introduction of cobalt–nickel into the catalysts leads to an increase in the activity of the catalysts. The method of low-temperature nitrogen adsorption actually makes it possible to estimate the size of the pores that are formed during the coordination of catalyst particles. Since these pores are formed by catalyst particles, the mathematical techniques used can be also used to determine the average particle size. Thus, the low-temperature nitrogen adsorption method is based on filling (adsorption) of the pores with liquid nitrogen. Prior to measurement, the sample is cooled to a temperature at which the transition from gaseous N_2 to the liquid phase occurs.

Table 5. Characteristics of mono- and bimetallic catalysts using the micrometry method.

Nomination	Co/Al_2O_4	Ni/Al_2O_4	Ni-$CoAl_2O_3$
Average particle size, nm	37.0355	944.33	874.8551
TEM, nm	620.55	1851	1071
Micropore volume: cm^3/g	0.004882	0.000279	0.000377
External surface area: m^2/g	147.9614	3.632	7.4253
Total surface area (BET): m^2/g	162.006	3.039	6.8583
Adsorption pore diameter (4V/A by BET), nm	12.205	16.19	22.054
Desorption pore diameter (4V/A by BET), nm	11.758	7.999	9.457

The size, volume, and surface area of catalysts are the most important characteristics to determine before and after the upgrading processes of heavy crude oil. Figures 13 and 14 show the BJH adsorption and desorption curves of the pore distribution of the Co/Al_2O_4 and Ni/Al_2O_4 catalysts. Additionally, Figure 15 presents the curves of BJH adsorption and desorption (pore volumes) of the Ni-$CoAl_2O_3$ catalyst. Although the catalysts were

synthesized by the same method, the large difference observed in the average sizes also depends on the composition of the catalysts, as can be seen in Table 4. These catalysts really have different sizes, where the average particle size is 37.0355, 944.33, and 874.8551 nm. In this article, we investigated the effect of cobalt, nickel, and the cobalt–nickel metal alloy on the refining process of extra-heavy oil. However, it is clear that the introduction of cobalt-nickel into the catalysts leads to an increase in the activity of the catalysts. According to TEM and SEM analysis, the average particle size of the Co/Al_2O_4, Ni/Al_2O_4, and $Ni\text{-}CoAl_2O_3$ catalysts is 0.62, 1.85, and 1.07 µm, respectively. According to the BJH curves, it should be indicated that for catalysts, pore diameters ranging from 10 to 60 nm have desorption values dropping from 0.00057 $cm^3/g{\cdot}nm$ to 0.00015 $cm^3/g{\cdot}nm$. Similarly, Figure 15 shows the BJH curves of adsorption and desorption of $Ni\text{-}CoAl_2O_3$. It has been observed that the diameter pores ranged from 6 to 80 nm of the catalyst, showing the pore volume value of 0.0009 $cm^3/g{\cdot}nm$, and the range of 80–120 nm showed from 0.0005 $cm^3/g{\cdot}nm$ to 0.0001$cm^3/g{\cdot}nm$ of the diameter pores.

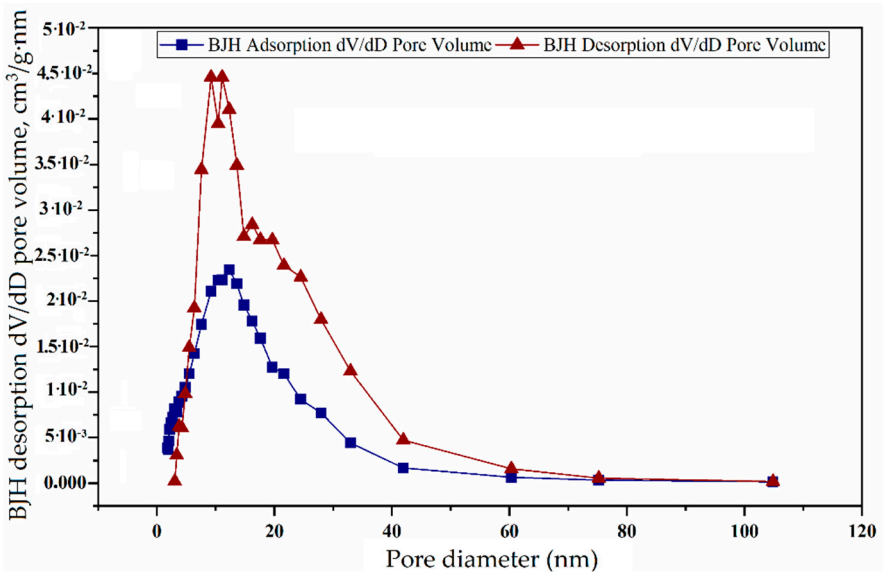


Figure 13. BJH adsorption and desorption of pore volume of Co/Al_2O_4 catalyst.

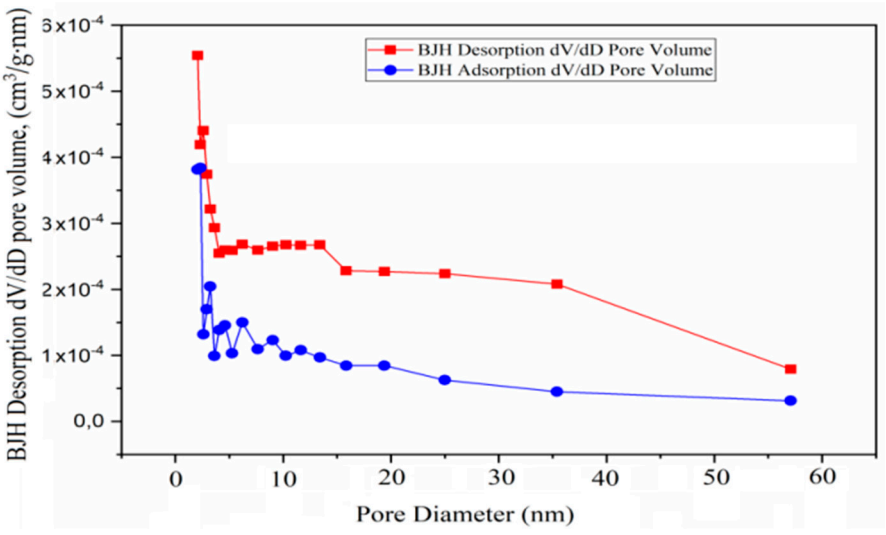


Figure 14. BJH adsorption and desorption of Ni/Al_2O_4 catalyst pore volume.

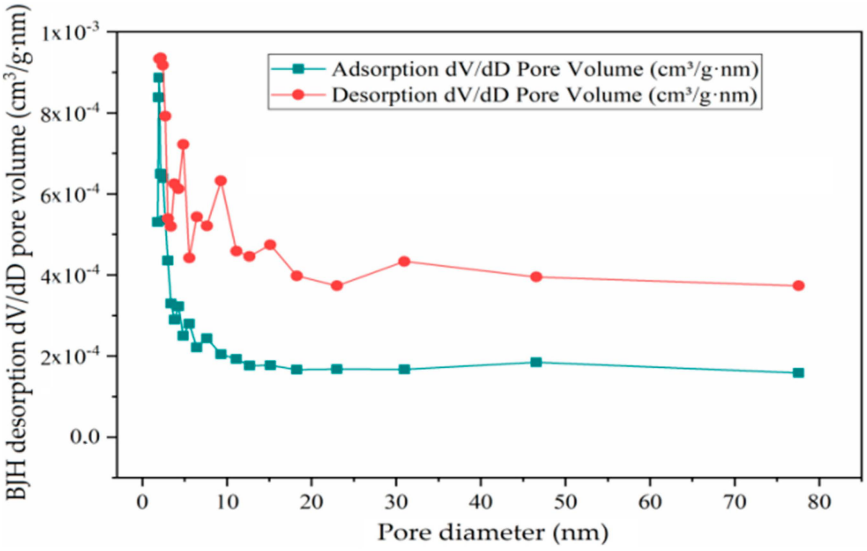


Figure 15. BJH adsorption and desorption of Ni-$CoAl_2O_3$ catalyst pore volume.

The obtained data from the surface area and volume pore analysis are summarized in Table 5.

3.5. Extra-Heavy Oil Hydrothermal Processing Experiments

Our experimental procedure of the thermocatalytic upgrading of extra-heavy oil in SCW was practically the same as the one proposed in our previous work [52]. The thermocatalytic experiments were performed at 420 ± 1 °C for 120 min (2 h) by inserting 75 ± 0.002 g of extra-heavy crude oil and 75 ± 0.002 g of distilled water into a high-pressure batch reactor under a static regime. Then, 2.00 wt.% of the investigated catalyst was added to the feedstock. An initial pressure of 5 bars at 25 °C was set in the reactor after removing air from the reactor by nitrogen injection. A detailed description of the separation procedure of gas–liquid–solid products can be found in our previous works. The terms S-0, S-1, S-2, S-3, S-4, and S-5 will be used to refer to the sample of extra-heavy crude oil (Tahe oil), sample without SCW, sample with SCW, sample with SCW + Co/Al_2O_4, sample with SCW + Ni/Al_2O_4, and sample with SCW + Ni-$CoAl_2O_3$, respectively.

4. Conclusions

A range of hydrogen production catalysts were synthesized and their effects on the hydrothermal upgrading of extra-heavy crude oil from the Chinese Tahe Oil Deposit were investigated. The acquired catalysts were characterized using a variety of physical and chemical ways before being used to upgrade the examined oil using various processing methods in the presence and absence of SCW. The examined catalysts had surface areas ranging from 3.04 to 162 m^2/g and average sizes ranging from 0.037 to 0.944 m. The yields of molecular hydrogen rose in the presence of SCW and catalysts, increasing from 1.0598 mol.% in the absence of SCW to 6.1320 mol.% in its presence, with a maximum yield of 11.78 mol.% in the presence of SCW and Ni-Co/Al_2O_3 catalysts. Furthermore, our findings demonstrate that the dramatic increase in hydrogen yields in the presence of SCW and catalysts is due to steam methane reforming and water–gas shift processes that occur throughout the upgrading process. Furthermore, the catalytic upgrading demonstrated a good performance for heteroatom removal via radical and oxidative processes, as evidenced by a decrease in sulfur from 1.84 to 1.35 wt.%. As a result, the viscosity of the improved oil samples fell from 61 × 10^6 mPas in the absence of SCW and catalysts to 3.72 mPas in their presence. Interestingly, SCW and catalytic upgrading performed well in the cleavage of C–C and C–H bonds in resin and asphaltene fractions, reducing the number of asphaltenes from 28% to 2%. Another benefit of SCW and the synthetized catalysts is a decrease in coke yield, which was found to reduce from 51.02 wt.% in the absence of SCW and catalysts to

33.64 wt.% in the presence of SCW, and to 17.08 wt.% in the presence of SCW and catalysts. The use of unconventional oil deposits and catalysts to solve the problem of hydrogen generation is already being researched. Our findings, we feel, are promising, and should be verified by broader applications.

Author Contributions: R.D.: conceptualization, data curation, investigation, editing, methodology, supervision, writing, and validation; I.R.I.: investigation and data curation; M.K.: investigation and data curation; M.A.K.: formal analysis, writing—editing and reviewing, and visualization; D.A.E.: investigation and data curation; A.A.A.-M.: data curation; M.A.S.: data curation; M.A.V.: writing, validation, funding acquisition, and supervision. All authors have read and agreed to the published version of the manuscript.

Funding: This research received no external funding.

Data Availability Statement: Not applicable.

Acknowledgments: This paper has been supported by the Kazan Federal University Strategic Academic Leadership Program (PRIORITY-2030).

Conflicts of Interest: The authors declare that there is no conflict of interest regarding the publication of this paper.

References

1. Sorin, F. World Energy Outlook 2006: The International Energy Agency (IEA) Report. *Rev. Gen. Nucl.* **2006**, 6–8.
2. *IEA Global Hydrogen Review 2021*; IEA: Paris, France, 2021.
3. Brandon, N.P.; Kurban, Z. Clean Energy and the Hydrogen Economy. *Philos. Trans. R. Soc. A Math. Phys. Eng. Sci.* **2017**, *375*, 20160400. [CrossRef] [PubMed]
4. Qyyum, M.A.; Dickson, R.; Shah, S.F.A.; Niaz, H.; Khan, A.; Liu, J.J.; Lee, M. Availability, Versatility, and Viability of Feedstocks for Hydrogen Production: Product Space Perspective. *Renew. Sustain. Energy Rev.* **2021**, *145*, 110843. [CrossRef]
5. Holladay, J.D.; Hu, J.; King, D.L.; Wang, Y. An Overview of Hydrogen Production Technologies. *Catal. Today* **2009**, *139*, 244–260. [CrossRef]
6. Kalamaras, C.M.; Efstathiou, A.M. Hydrogen Production Technologies: Current State and Future Developments. In *Proceedings of the Conference Papers in Science*; Hindawi: London, UK, 2013; Volume 2013.
7. Song, C. Fuel Processing for Low-Temperature and High-Temperature Fuel Cells: Challenges, and Opportunities for Sustainable Development in the 21st Century. *Catal. Today* **2002**, *77*, 17–49. [CrossRef]
8. McHugh, K.; Eisele, S.; Nestell, J. *Hydrogen Production Methods*; MPRWP-0001; MPR Associates. Inc.: Alexandria, VI, USA, 2005.
9. Bian, Z.; Wang, Z.; Jiang, B.; Hongmanorom, P.; Zhong, W.; Kawi, S. A Review on Perovskite Catalysts for Reforming of Methane to Hydrogen Production. Renew. *Sustain. Energy Rev.* **2020**, *134*, 110291. [CrossRef]
10. Krummenacher, J.J.; West, K.N.; Schmidt, L.D. Catalytic Partial Oxidation of Higher Hydrocarbons at Millisecond Contact Times: Decane, Hexadecane, and Diesel Fuel. *J. Catal.* **2003**, *215*, 332–343. [CrossRef]
11. Steinberg, M. A Highly Efficient Combined Cycle Fossil and Biomass Fuel Cell Power Generation and Hydrogen Production Plant with Zero CO_2 Emission. In Proceedings of the International Conference on Fuel Cell Science, Engineering and Technology, Kyiv, Ukraine, 6–10 June 2004; Volume 41650, pp. 401–408.
12. Chum, H.L.; Overend, R.P. Biomass and Renewable Fuels. *Fuel Process. Technol.* **2001**, *71*, 187–195. [CrossRef]
13. Demirbas, A. Combustion Characteristics of Different Biomass Fuels. *Prog. Energy Combust. Sci.* **2004**, *30*, 219–230. [CrossRef]
14. Holladay, J.D.; Wang, Y.; Jones, E. Review of Developments in Portable Hydrogen Production Using Microreactor Technology. *Chem. Rev.* **2004**, *104*, 4767–4790. [CrossRef]
15. Weingärtner, H.; Franck, E.U. Supercritical Water as a Solvent. *Angew. Chemie Int. Ed.* **2005**, *44*, 2672–2692. [CrossRef] [PubMed]
16. Hayashi, H.; Hakuta, Y. Hydrothermal Synthesis of Metal Oxide Nanoparticles in Supercritical Water. *Materials* **2010**, *3*, 3794–3817. [CrossRef] [PubMed]
17. Wu, Z.; Ren, Y.; Ou, G.; Jin, H. Influence of Special Water Properties Variation on the Heat Transfer of Supercritical Water Flow around a Sphere. *Chem. Eng. Sci.* **2020**, *222*, 115698. [CrossRef]
18. Fois, E.S.; Sprik, M.; Parrinello, M. Properties of Supercritical Water: An Ab Initio Simulation. *Chem. Phys. Lett.* **1994**, *223*, 411–415. [CrossRef]
19. Okolie, J.A.; Nanda, S.; Dalai, A.K.; Berruti, F.; Kozinski, J.A. A Review on Subcritical and Supercritical Water Gasification of Biogenic, Polymeric and Petroleum Wastes to Hydrogen-Rich Synthesis Gas. *Renew. Sustain. Energy Rev.* **2020**, *119*, 109546. [CrossRef]
20. Antipenko, V.R.; Fedyaeva, O.N.; Grin'ko, A.A.; Vostrikov, A.A. Structural Group Characteristics of Resins and Asphaltenes of High-Sulfur Natural Asphaltite and Products of Its Conversion in Supercritical Water. *Pet. Chem.* **2020**, *60*, 668–674. [CrossRef]

21. Cocero, M.J.; Calvo, L. Supercritical Fluid Extraction of Sunflower Seed Oil with CO2-ethanol Mixtures. *J. Am. Oil Chem. Soc.* **1996**, *73*, 1573–1578. [CrossRef]
22. Bruges, E.A.; Gibson, M.R. Dynamic Viscosity of Compressed Water to 10 Kilobar and Steam to 1500 C. *J. Mech. Eng. Sci.* **1969**, *11*, 189–205. [CrossRef]
23. Yoshii, N.; Miura, S.; Okazaki, S. A Molecular Dynamics Study of Dielectric Constant of Water from Ambient to Sub-and Supercritical Conditions Using a Fluctuating-Charge Potential Model. *Chem. Phys. Lett.* **2001**, *345*, 195–200. [CrossRef]
24. Redelius, P. Bitumen Solubility Model Using Hansen Solubility Parameter. *Energy Fuels* **2004**, *18*, 1087–1092. [CrossRef]
25. Chham, A.; Khouya, E.; Abourriche, A.K.; Oumam, M.; Gmouh, S.; Mansouri, S.; El Harti, M.; Hannache, H. Supercritical Water Extraction and Characterization of Moroccan Shale Oil by Different Solvent. *J. Mater. Environ. Sci.* **2018**, *9*, 1771–1778.
26. Duan, P.-G.; Yang, S.-K.; Xu, Y.-P.; Wang, F.; Zhao, D.; Weng, Y.-J.; Shi, X.-L. Integration of Hydrothermal Liquefaction and Supercritical Water Gasification for Improvement of Energy Recovery from Algal Biomass. *Energy* **2018**, *155*, 734–745. [CrossRef]
27. Sitnov, S.A.; Khelkhal, M.A.; Mukhamatdinov, I.I.; Feoktistov, D.A.; Vakhin, A.V. Iron Oxide Nanoparticles Impact on Improving Reservoir Rock Minerals Catalytic Effect on Heavy Oil Aquathermolysis. *Fuel* **2022**, *327*, 124956. [CrossRef]
28. Farhadian, A.; Khelkhal, M.A.M.A.; Tajik, A.; Lapuk, S.E.S.E.; Rezaeisadat, M.; Eskin, A.A.A.A.; Rodionov, N.O.N.O.; Vakhin, A.V.A.V. Effect of Ligand Structure on the Kinetics of Heavy Oil Oxidation: Toward Biobased Oil-Soluble Catalytic Systems for Enhanced Oil Recovery. *Ind. Eng. Chem. Res.* **2021**, *60*, 14713–14727. [CrossRef]
29. Pan, Y.; Abazari, R.; Wu, Y.; Gao, J.; Zhang, Q. Advances in Metal–Organic Frameworks and Their Derivatives for Diverse Electrocatalytic Applications. *Electrochem. Commun.* **2021**, *126*, 107024. [CrossRef]
30. Barbaro, P.; Liguori, F. *Heterogenized Homogeneous Catalysts for Fine Chemicals Production: Materials and Processes*; Springer: Berlin/Heidelberg, Germany, 2010; Volume 33, ISBN 9048136962.
31. Zalesskiy, S.S.; Ananikov, V.P. Pd2 (Dba) 3 as a Precursor of Soluble Metal Complexes and Nanoparticles: Determination of Palladium Active Species for Catalysis and Synthesis. *Organometallics* **2012**, *31*, 2302–2309. [CrossRef]
32. Bahrami, F.; Panahi, F.; Daneshgar, F.; Yousefi, R.; Shahsavani, M.B.; Khalafi-Nezhad, A. Synthesis of New α-Aminophosphonate Derivatives Incorporating Benzimidazole, Theophylline and Adenine Nucleobases Using l-Cysteine Functionalized Magnetic Nanoparticles (LCMNP) as Magnetic Reusable Catalyst: Evaluation of Their Anticancer Properties. *RSC Adv.* **2016**, *6*, 5915–5924. [CrossRef]
33. Lin, L.; Jiang, W.; Chen, L.; Xu, P.; Wang, H. Treatment of Produced Water with Photocatalysis: Recent Advances, Affecting Factors and Future Research Prospects. *Catalysts* **2020**, *10*, 924. [CrossRef]
34. Tada, S.; Shimizu, T.; Kameyama, H.; Haneda, T.; Kikuchi, R. Ni/CeO2 Catalysts with High CO2 Methanation Activity and High CH4 Selectivity at Low Temperatures. *Int. J. Hydrogen Energy* **2012**, *37*, 5527–5531. [CrossRef]
35. Wu, Y.; Li, Y.; Gao, J.; Zhang, Q. Recent Advances in Vacancy Engineering of Metal-organic Frameworks and Their Derivatives for Electrocatalysis. *SusMat* **2021**, *1*, 66–87. [CrossRef]
36. Hossain, M.M. Upgrading of Heavy Oil in Supercritical Water Using an Iron Based Multicomponent Catalyst. *Int. J. Chem. React. Eng.* **2017**, *15*, 161–167. [CrossRef]
37. Duan, P.; Savage, P.E. Upgrading of Crude Algal Bio-Oil in Supercritical Water. *Bioresour. Technol.* **2011**, *102*, 1899–1906. [CrossRef] [PubMed]
38. Remón, J.; Arauzo, J.; García, L.; Arcelus-Arrillaga, P.; Millan, M.; Suelves, I.; Pinilla, J.L. Bio-Oil Upgrading in Supercritical Water Using Ni-Co Catalysts Supported on Carbon Nanofibres. *Fuel Process. Technol.* **2016**, *154*, 178–187. [CrossRef]
39. You, X.; Wang, X.; Ma, Y.; Liu, J.; Liu, W.; Xu, X.; Peng, H.; Li, C.; Zhou, W.; Yuan, P. Ni-Co/Al2O3 Bimetallic Catalysts for CH4 Steam Reforming: Elucidating the Role of Co for Improving Coke Resistance. *ChemCatChem* **2014**, *6*, 3377–3386. [CrossRef]
40. Nyankson, E.; Efavi, J.K.; Yaya, A.; Manu, G.; Asare, K.; Daafuor, J.; Abrokwah, R.Y. Synthesis and Characterisation of Zeolite-A and Zn-Exchanged Zeolite-A Based on Natural Aluminosilicates and Their Potential Applications. *Cogent. Eng.* **2018**, *5*, 1440480. [CrossRef]
41. Hosseinpour, M.; Fatemi, S.; Ahmadi, S.J.; Morimoto, M.; Akizuki, M.; Oshima, Y.; Fumoto, E. The Synergistic Effect between Supercritical Water and Redox Properties of Iron Oxide Nanoparticles during In-Situ Catalytic Upgrading of Heavy Oil with Formic Acid. Isotopic Study. *Appl. Catal. B Environ.* **2018**, *230*, 91–101. [CrossRef]
42. Dejhosseini, M.; Aida, T.; Watanabe, M.; Takami, S.; Hojo, D.; Aoki, N.; Arita, T.; Kishita, A.; Adschiri, T. Catalytic Cracking Reaction of Heavy Oil in the Presence of Cerium Oxide Nanoparticles in Supercritical Water. *Energy Fuels* **2013**, *27*, 4624–4631. [CrossRef]
43. Yeletsky, P.M.; Reina, T.R.; Bulavchenko, O.A.; Saraev, A.A.; Gerasimov, E.Y.; Zaikina, O.O.; Bermúdez, J.M.; Arcelus-Arrillaga, P.; Yakovlev, V.A.; Millan, M. Phenanthrene Catalytic Cracking in Supercritical Water: Effect of the Reaction Medium on NiMo/SiO2 Catalysts. *Catal. Today* **2019**, *329*, 197–205. [CrossRef]
44. Vogelaar, B.M.; Makkee, M.; Moulijn, J.A. Applicability of Supercritical Water as a Reaction Medium for Desulfurisation and Demetallisation of Gasoil. *Fuel Process. Technol.* **1999**, *61*, 265–277. [CrossRef]
45. Patwardhan, P.R.; Timko, M.T.; Class, C.A.; Bonomi, R.E.; Kida, Y.; Hernandez, H.H.; Tester, J.W.; Green, W.H. Supercritical Water Desulfurization of Organic Sulfides Is Consistent with Free-Radical Kinetics. *Energy Fuels* **2013**, *27*, 6108–6117. [CrossRef]
46. Carvalho, L.S.; Martins, A.R.; Reyes, P.; Oportus, M.; Albonoz, A.; Vicentini, V.; do Carmo Rangel, M. Preparation and Characterization of Ru/MgO-Al2O3 Catalysts for Methane Steam Reforming. *Catal. Today* **2009**, *142*, 52–60. [CrossRef]

47. Gangadharan, P.; Kanchi, K.C.; Lou, H.H. Evaluation of the Economic and Environmental Impact of Combining Dry Reforming with Steam Reforming of Methane. *Chem. Eng. Res. Des.* **2012**, *90*, 1956–1968. [CrossRef]
48. Oyama, S.T.; Hacarlioglu, P.; Gu, Y.; Lee, D. Dry Reforming of Methane Has No Future for Hydrogen Production: Comparison with Steam Reforming at High Pressure in Standard and Membrane Reactors. *Int. J. Hydrog. Energy* **2012**, *37*, 10444–10450. [CrossRef]
49. Olah, G.A.; Goeppert, A.; Czaun, M.; Prakash, G.K.S. Bi-Reforming of Methane from Any Source with Steam and Carbon Dioxide Exclusively to Metgas (CO–2H2) for Methanol and Hydrocarbon Synthesis. *J. Am. Chem. Soc.* **2013**, *135*, 648–650. [CrossRef] [PubMed]
50. Morimoto, M.; Sugimoto, Y.; Saotome, Y.; Sato, S.; Takanohashi, T. Effect of Supercritical Water on Upgrading Reaction of Oil Sand Bitumen. *J. Supercrit. Fluids* **2010**, *55*, 223–231. [CrossRef]
51. Hart, A.; Omajali, J.B.; Murray, A.J.; Macaskie, L.E.; Greaves, M.; Wood, J. Comparison of the Effects of Dispersed Noble Metal (Pd) Biomass Supported Catalysts with Typical Hydrogenation (Pd/C, Pd/Al2O3) and Hydrotreatment Catalysts (CoMo/Al2O3) for in-Situ Heavy Oil Upgrading with Toe-to-Heel Air Injection (THAI). *Fuel* **2016**, *180*, 367–376. [CrossRef]
52. Djimasbe, R.; Varfolomeev, M.A.; Al-Muntaser, A.A.; Yuan, C.; Feoktistov, D.A.; Suwaid, M.A.; Kirgizov, A.J.; Davletshin, R.R.; Zinnatullin, A.L.; Fatou, S.D. Oil Dispersed Nickel-Based Catalyst for Catalytic Upgrading of Heavy Oil Using Supercritical Water. *Fuel* **2021**, *313*, 122702. [CrossRef]
53. Djimasbe, R.; Varfolomeev, M.A.; Al-Muntaser, A.A.; Yuan, C.; Suwaid, M.A.; Feoktistov, D.A.; Rakhmatullin, I.Z.; Milovankin, A.A.; Murzakhanov, F.; Morozov, V. Deep Insights into Heavy Oil Upgrading Using Supercritical Water by a Comprehensive Analysis of GC, GC–MS, NMR, and SEM–EDX with the Aid of EPR as a Complementary Technical Analysis. *ACS Omega* **2021**, *6*, 135–147. [CrossRef]
54. Djimasbe, R.; Varfolomeev, M.A.; Al-Muntasser, A.A.; Suweid, M.A.; Osin Yu, N.; Diop, F.S.; Mustafina, A.N.; Garaeva, D.I. Upgrading of Heavy Oil under the Exposition of Supercritical Water at Different Temperatures. *Октябрь* **2018**. [CrossRef]
55. Rakhmatullin, I.; Efimov, S.; Tyurin, V.; Gafurov, M.; Al-Muntaser, A.; Varfolomeev, M.; Klochkov, V. Qualitative and Quantitative Analysis of Heavy Crude Oil Samples and Their SARA Fractions with ^{13}C Nuclear Magnetic Resonance. *Processes* **2020**, *8*, 995. [CrossRef]
56. Yen, T.F.; Erdman, J.G.; Pollack, S.S. Investigation of the Structure of Petroleum Asphaltenes by X-Ray Diffraction. *Anal. Chem.* **1961**, *33*, 1587–1594. [CrossRef]